Chem. Mater. **2000,** *12,* 501−510

Thermal Behavior of 12-Molybdophosphoric Acid Supported on Zirconium-Loaded Silica

S. Damyanova,[†] L. M. Gomez,[‡] M. A. Bañares,[‡] and J. L. G. Fierro*,[‡]

Institute of Catalysis, Bulgarian Academy of Science, 1113 Sofia, Bulgaria, and Instituto de Catálisis y Petroleoquímica, CSIC, Campus UAM, Cantoblanco, 28049, Madrid, Spain

Received August 31, 1999

The thermal behavior of 12-molybdophosphoric acid (HPMo) supported on silica and Zr-loaded silica (Zr content from 1.6 to 17.0 wt %) was studied by X-ray diffraction, Fourier-transform infrared, in situ Raman, and X-ray photoelectron spectroscopic techniques. A silica support stabilizes the Keggin unit of HPMo up to 773 K, which is ca. 100 K higher than the unsupported one. For the Zr(1.6)SiO_2 support at 773 K, the thermal stability of HPMo is similar to that of the silica-supported counterpart. For Zr contents above 5.6 wt %, decomposition of HPMo occurs at lower temperatures, and this is accompanied by the formation of structure analogues of $Zr(MoO_4)_2$. While $Zr(x)SiO_2$ supports stabilize surface molybdenum oxide species, silica is unable to spread molybdena, which segregates like bulk MoO_3. The interactions of the Mo−Zr oxide species appear to be responsible for the activity enhancement in methanol oxidation. The marked decrease of the dimethyl ether/formaldehyde selectivity ratio with increasing zirconium content on the samples calcined at 723 K indicates that the redox function of the interaction of Mo−Zr species increases formaldehyde selectivity.

1. Introduction

The catalytic function of heteropoly compounds has attracted increasing attention during the past years due to their variety and high potential as catalyst.[1,2] The heteropoly compounds (HPC) with a Keggin structure have been the catalysts most widely investigated because of their stability and ease of synthesis. Many previous works have reported results in the application of heteropoly acids as new materials, especially as a proton conductors and antistatic films and in the conversion of solar energy. Additionally, they can be used in solution as well as in the solid state as acid and oxidation catalysts.

Heteropoly compounds have been studied as bulk catalysts as well as in supported form. The deposition of heteropoly acids onto solid supports with high area is important for catalytic applications because the area of unsupported ones is low. Moreover, the problem of the thermal stability of supported HPC is also very important, because the temperature of the catalytic reaction usually lies within the temperature range of their decomposition. The temperature for the decomposition of the Keggin structure depends on the heteroatom (Si or P), the metal atom (W or Mo), or the type of the support. Several supports such as silica, kieselguhr, or carbon have been used.[3−9] It has been shown that heteropoly acids supported on alumina and MgO,[10−13] having basicity, are decomposed during their preparation. SiO_2-supported heteropoly compounds such as $H_4SiMo_{12}O_{40}$, $H_3PMo_{12}O_{40}$, and $H_5PMo_{10}V_2O_{40}$ partly decompose at very low loading due to their strong interactions with surface silanol groups.[14−16] It has been observed[7,15] that silica induces the destabilization of 12-molybdosilicic and 12-molybdophosphoric acid and that their thermal stability is reduced by 20−30 K compared to their unsupported counterparts. Destruction of the Keggin unit (KU) of 12-molybdophosphate[15] and 12-molybdosilicate[17] anions begins at about 573 and 623 K, respectively. In contrast, it has been concluded[8,18] that the silicomolybdate and the molybdophosphate anion on the silica support are thermally stable up to 873 K. Recently, we have observed that titania improves

---

* Fax: +34 91 585 4760. Telephone: +34 91 585 4769. E-mail: jlgfierro@icp.csic.es.

[†] Bulgarian Academy of Science.

[‡] CSIC.

(1) Kozhevnikov, Y. V. *Chem. Rev.* **1998**, *98*, 171.

(2) Mizuno, M.; Misono, M. *Chem. Rev.* **1998**, *98*, 199.

(3) Ai, M. *J. Catal.* **1981**, *71*, 88.

(4) Baba, T.; Ono, T.; Ishimoto, S.; Morikawa, S.; Tanooka, S. *Bull. Chem. Soc. Jpn.* **1985**, *58*, 2155.

(5) Izumi, Y.; Hasehe, R.; Urabe, K. *J. Catal.* **1983**, *84*, 402.

(6) Izumi, Y.; Urabe, K. *Chem. Lett.* **1981**, 663.

(7) Rocchiccioli-Deltcheff, C.; Aouissi, A.; Bettahar, M.; Launay, S.; Fournier, M. *J. Catal.* **1996**, *164*, 16.

(8) Kasztelan, S.; Payen, E.; Moffat, J. B. *J. Catal.* **1990**, *125*, 45.

(9) Schwegler, M. A.; van Bekkum, H.; de Munok, N. A. *Appl. Catal.* **1992**, *80*, 92.

(10) Luthra, N. P.; Cheng, W. C. *J. Catal.* **1988**, *109*, 163.

(11) Nowinska, K.; Fiedorow, R.; Adamiec, J. *J. Chem. Soc., Faraday Trans.* **1991**, *87*, 749.

(12) Rao, K. M.; Gobetto, R.; Iannibello, A.; Zecchina, A. *J. Catal.* **1989**, *119*, 512.

(13) van Veen, J. A. R.; Hendriks, P. A. J. M.; Andrea, R. R.; Romers, E. J. M.; Wilson, A. E. *J. Phys. Chem.* **1990**, *94*, 1831.

(14) Brückman, K.; Che, M.; Haber, J.; Tatibouet, J. M. *Catal. Lett.* **1994**, *25*, 225.

(15) Rocchiccioli-Deltcheff, C.; Amirouche, M.; Herve, G.; Fournier, M.; Che, M.; Tatibouet, J. M. *J. Catal.* **1990**, *126*, 591.

(16) Tatibouet, J. M.; Montaleskcot, C.; Brückman, E.; Haber, J.; Che, M. *J. Catal.* **1997**, *169*, 22.

(17) Bañares, M. A.; Hangchun, H.; Wachs, I. E. *J. Catal.* **1995**, *155*, 249.

(18) Goncharova, O. I.; Davydov, A. A.; Yurieva, T. M.; Khochireva, T. Kh. *Kinet. Katal.* **1983**, *24*, 576.

10.1021/cm9911316 CCC: $19.00

Table 1. Chemical Analysis and Specific Areas of the Catalysts

catalyst	Zr (wt %)	Mo (wt %)	S_{BET} (m^2/g)
HPMo/SiO_2		23.8	185
HPMo/Zr(1.6)SiO_2	1.6	22.7	194
HPMo/Zr(5.6)SiO_2	5.6	22.4	203
HPMo/Zr(9.6)SiO_2	9.6	23.2	184
HPMo/Zr(17.0)SiO_2	17.0	21.7	159

the thermal stability of supported 12-molybdophosphoric acid and its Co and Ni salts up to temperature higher than that of the unsupported compound.[19]

Insight into the transformation of HPC into oxide on different supports is important for controlling the nature of the active oxide phase obtained after thermal decomposition of supported HPC species. It can be therefore expected that a well-dispersed oxide phase or surface oxide species could be formed after thermal decomposition of HPC. All of this depends on the interaction between deposited surface species and the support. From this point of view, in the present work, we report a detailed study of the thermal behavior of 12-molybdophosphoric acid (HPMo) supported on silica and silica-zirconium substrates. Zirconium oxide was assumed to play the role of a basic site able to form strong interactions between them and acid HPMo. To investigate the decomposition mechanism of supported HPMo, different techniques have been used, including X-ray diffraction (XRD), in situ Raman, IR, and X-ray photoelectron spectroscopies (XPS) and catalytic activity in methanol oxidation.

2. Experimental Section

2.1. Sample Preparation. Zirconium-loaded silica supports were prepared by impregnation of silica with zirconium *n*-propoxide in *n*-propanol.[20] The supports were dried at 383 K for 12 h and calcined in air at 773 K for 7 h. Four mixed supports containing 1.6, 5.6, 9.6, and 17.0 wt % Zr were prepared. Hereafter, the samples are referred to as Zr(x)SiO_2, where x denotes the weight percent of Zr. Supported-HPMo catalysts were prepared by the wetness impregnation method of SiO_2 and Zr(x)SiO_2 supports. The desired amount of 12-molybdophosphoric acid (Aldrich, reagent grade) was dissolved in distilled water, and the solution was mixed with the solid. The resulting solid was dried at 383 K and calcined at different temperatures of 473−923 K for 2 h. The composition, as measured by atomic absorption spectroscopy, and specific area of the samples are summarized in Table 1.

2.2. Characterization. Molybdenum content was determined using a Perkin-Elmer 3030 atomic absorption spectrophotometer, following acid digestion of the samples. The powder X-ray diffraction patterns of the samples were recorded on a Seifert 3000P diffractometer with nickel-filtered Cu Kα ($\lambda = 0.15418$ nm) radiation by scanning 2Θ angles ranging from 5 to 75°.

Photoelectron spectra (XPS) were acquired with a VG ESCALAB 200R spectrometer equipped with a hemispherical electron analyzer and an Mg Kα ($h\nu = 1253.6$ eV, 1 eV $= 1.603 \times 10^{-19}$ J) 120 W X-ray source. The powder samples were pressed into small stainless steel cylinders and then mounted on a heater placed in the pretreatment chamber. Prior to being moved into the analysis chamber, the samples were evacuated in the pretreatment chamber of the instrument at room temperature. The residual pressure in the ion-pumped analysis chamber was maintained below 5×10^{-9} Torr during data acquisition. The intensities of Mo 3d, P 2p, Zr 3d, O 1s, and Si 2p peaks were estimated by calculating the integral of the peaks after smoothing and subtraction of the "S-shaped" background and fitting the experimental curve to a combination of Gaussian and Lorentzian lines. The binding energies (BE) were referenced to the C 1s peak at 284.9 eV; this reference affording BE values with an accuracy of ±0.1 eV.

Framework vibration spectra in the 1200−400 cm^{-1} range were recorded on a FTIR Nicolet 5 ZDX spectrophotometer working at a resolution of 4 cm^{-1} and averaged over 100 scans. Self-supporting wafers were prepared by pelleting the samples 1:100 diluted in KBr. The Raman spectra were run with a single Renishaw system 1000 monochromator equipped with a cooled CCD detector (200 K) and a holographic Notch filter, which affords higher Raman signals than are obtained with triple monochromator spectrometers. The samples were excited with the 514 nm Ar line in an in situ treatment cell (Linkam, TS-1500), permitting temperature treatments under flowing gases (dry air). The spectral resolution was better than 2 cm^{-1}, and spectrum acquisition consisted of five accumulations of 60 s. To ensure ambient conditions, the air stream passed through a saturator to simulate ambient humidity. It should be noted that the bulk HPMo was very easily decomposed under the power of the laser beam (25 mW) even at room temperature. Decomposition led to the formation of MoO_3, detected by its strong Raman band at 820 and 998 cm^{-1}. This was not the case with supported HPMo samples because the same spectra were obtained at increasing beam power at specific temperatures. Thus, the spectra were run under 25 mW for supported samples and 2.5 mW for bulk HPMo.

2.3. Activity Measurements. Catalytic experiments were performed in a continuous-flow tubular reactor (6.2 mm ID) using 0.040 g of catalyst. A CH_3OH:O_2:He (=5:10:85 molar ratio) mixture was fed into the reactor at a total flow 100 cm^3 min^{-1}. Liquid methanol (0.5 cm^3 h^{-1}) was fed by means of a liquid pump (Bencton-Dickinson) and then vaporized prior to the reactor inlet. The products were analyzed by an on-line gas chromatograph (Varian 3400 CX) provided with a thermoconductivity detector and a Porapak Q packed column. Pretreatment of the samples was done in the reactor in a flow of O_2:He (=10:90 molar ratio) prior to each run.

3. Results

3.1. XPS Measurements. The BEs of core electrons and surface atomic ratios were measured for samples subjected to different calcination temperatures. The BE values of Mo $3d_{5/2}$, Zr $3d_{5/2}$, and P 2p core levels of the samples subjected to calcination temperatures between 383 and 723 K are summarized in Table 1. The BE of the P 2p core level remained virtually unchanged for samples pretreated at 383 K. However, substantial changes occurred upon calcination at higher temperatures as a consequence of the decomposition of the heteropolyanion. Despite this, in the presence of zirconia, phosphorus tended to disperse in the bulk of the carrier because the signal was almost undetectable using XPS. The observation of two components in the Mo $3d_{5/2}$ core levels at ca. 232.4 and 233.6 eV for HPMo supported on SiO_2 and Zr(5.6)SiO_2 supports suggests the presence of Mo^{6+} species in different oxo−molybdenum compounds. The difference in the values of BE of Mo $3d_{5/2}$ level for SiO_2- and Zr(x)SiO_2-supported samples means that the coordination number of Mo is different, due to a different bonding strength between the molybdenum oxide species and the supports. The fact that BE of Zr $3d_{5/2}$ (182.5−182.7 eV) for all samples was higher than that of bulk ZrO_2 (182.1 eV) can be understood by assuming that the coordination number of zirconium on the silica surface is different from the situation in the bulk structure of ZrO_2. As will be seen below from the

---

(19) Damyanova, S.; Fierro, J. L. G. *Chem. Mater.* **1998**, *10*, 871

(20) Damyanova, S.; Grange, P.; Delmon, B. *J. Catal.* **1997**, *168*, 421.

Table 2. Binding Energies (eV) of Core Electrons of Samples HPMo/Zr(x)SiO$_2$ Subjected to Different Calcination Temperatures

sample	P 2p	Mo 3d$_{5/2}$	Zr 3d$_{5/2}$
	383 K		
PMo/SiO$_2$	133.7	232.4(71)[a] 233.7(29)	
PMo/Zr(5.6)SiO$_2$	133.7	232.5(75) 233.5(25)	182.7
PMo/Zr(17.0)SiO$_2$	132.8	232.5	182.4
	523 K		
PMo/SiO$_2$		232.2	
PMo/Zr(5.6)SiO$_2$		232.8	182.8
PMo/Zr(9.6)SiO$_2$		232.9	182.8
PMo/Zr(17.0)SiO$_2$		232.8	182.7
	623 K		
PMo/SiO$_2$	133.3	232.1	
PMo/Zr(5.6)SiO$_2$		232.7	182.5
PMo/Zr(9.6)SiO$_2$		232.6	182.7
PMo/Zr(17.0)SiO$_2$		232.7	182.5
	723 K		
PMo/SiO$_2$	133.4	232.0	
PMo/Zr(5.6)SiO$_2$		232.8	182.7
PMo/Zr(9.6)SiO$_2$		232.7	182.8
PMo/Zr(17.0)SiO$_2$		232.8	182.6

[a] Peak percentages in parentheses.

XRD and Raman spectra, the formation of different compounds with molybdenum or phosphates might well be involved. It should be noted that in Zr(x)SiO$_2$ carriers a close interaction between zirconia and silica via Zr−O−Si linkages has been reported.[20]

The values of the XPS Mo/Zr(Si) atomic ratios as a function of the zirconium content and pretreatment temperature are compiled in Table 2. For the HPMo/SiO$_2$ sample, the XPS Mo/Si ratios increase by a factor of approximately 3 with increasing temperature from 383 to 723 K. It means that the heteropolyanion clusters break up upon heating and the molybdenum oxide species disperse on the silica surface. Therefore, the higher XPS Mo/Si ratio for silica-supported sample at 723 K suggests a higher dispersion of molybdenum species. The addition of small amounts of zirconium (5.6−9.6%) did not strongly alter the XPS Mo/(Zr + Si) atomic ratios as compared to that of silica-supported HPMo in the low-temperature range of 383−623 K. However, at 723 K, the atomic ratio is roughly half that found in the Zr-free counterpart. The latter observation is consistent with the breaking up of the large polymolybdate aggregates and the formation of new ones when the calcination temperature is increased. The very slight change in the XPS Mo/(Zr + Si) atomic ratio with the calcination temperature for the sample with the highest Zr loading suggests a strong interaction between zirconia and molybdenum oxide species. Additionally, this interaction can be supported by a decrease of the XPS Zr/Si atomic ratio for each sample with increasing the temperature. Finally, the almost complete disappearance of phosphorus from samples calcined at temperatures above 523 K, specifically for the Zr-containing samples, suggests that phosphate ions generated when the KU is broken diffuse into the bulk of the Zr(x)SiO$_2$ carriers.

3.2. XRD Measurements. Figure 1A shows the XRD patterns of bulk HPMo subjected to different calcination temperatures. The pattern of the unpretreated HPMo (Figure 1A, line a) is typical for heteropoly acid.[21,22] Upon pretreatment at 383, the pattern differs significantly from the previous one, and no further change was observed upon calcination at 523 K. This range of 383−523 K corresponds to the loss of crystallization water, and it is related to the formation of the anhydrous acid phase.[19] A change in the XRD pattern was observed upon calcination at 623 K: the peaks belonging to that phase disappeared and new diffraction peaks appeared. These differed from the pattern of the anhydrous phase not only in a shift of the reflections but also in the distribution of their intensities. The lines at 623 K would be assigned to the formation of a mixture of orthorhombic α-MoO$_3$[7,23] and monoclinic β-MoO$_3$, reported as a structural analogue of WO$_3$,[7,23−25] where the

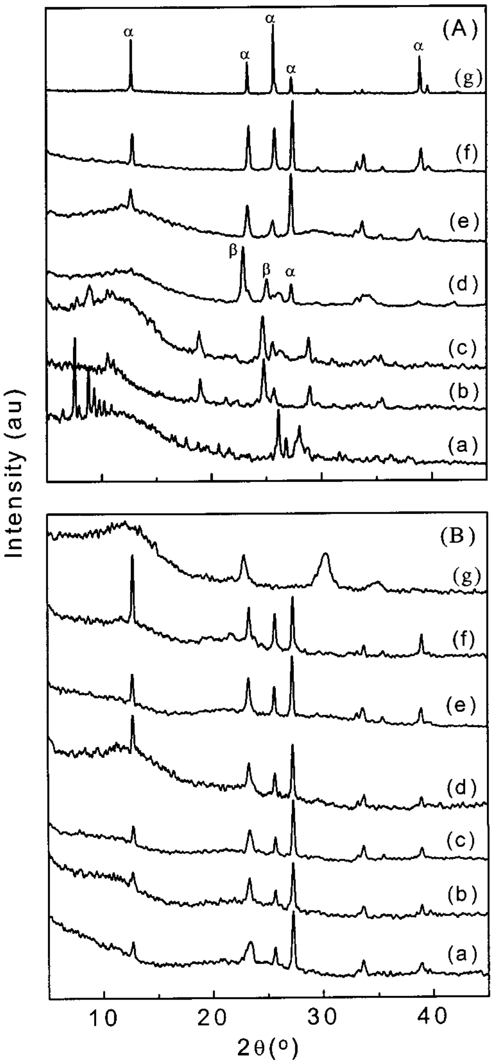

Figure 1. XRD patterns of bulk HPMo (A) and supported samples (B): HPMo/SiO$_2$ (a, c, e), HPMo/Zr(1.6)SiO$_2$ (b, d, f), and HPMo/Zr(17.0)SiO$_2$ (g) at different temperature treatments. Part A was read at (a) 298, (b) 383, (c) 523, (d) 623, (e) 723, (f) 823, and (g) 923 K. Part B was read at (a, b) 623, (c, d) 723, (e, f) 823, and (g) 923 K.

---

(21) Black, J. B.; Clayden, N. J.; Gai, P. L.; Serwicka, E. M.; Goodenough, J. B. *J. Catal.* **1987**, *106*, 1.

(22) Bondareva, V. M.; Andrushkevich, T. V.; Maksimovskaya, R. Y.; Plyasova, L. M.; Ziborov, A. V.; Litvak, G. S.; Detusheva, L. G. *Kinet. Katal.* **1994**, *35*, 114.

(23) Westman, S.; Magneli, A. *Acta Chem. Scand.* **1957**, *11*, 1587.

(24) McCarron, E. M. *J. Chem. Soc., Chem. Commun.* **1986**, 336.

β-MoO_3 phase dominates. α-MoO_3 phase begins to predominate at treatment temperatures above 723 K. The difference in the color of β-(yellow) and α-(white) MoO_3 can also be assigned to the structural dissimilarity between the two phases. The X-ray diffraction patterns of the sample calcined at 823−923 K were practically the same with a change in the relative intensities of the peaks, corresponding to the formation of bulk α-MoO_3.

The XRD patterns of HPMo supported on SiO_2 and Zr(x)SiO_2 supports calcined at various temperatures (Figure 1B) confirm the different types of behavior of these samples. The diffraction patterns of supported samples up to 573 K are characterized by an overall poor crystallinity, the lack of sharp reflections of the above-defined phases, and a broad amorphous background, indicating the presence of a noncrystalline phase. A pattern of α-MoO_3, in addition to minor lines due to β-MoO_3, is present in the pattern of HPMo/SiO_2 at 623 K (Figure 1Bb), but it is not present on HPMo/Zr(1.6)-SiO_2. The lines characteristic of α-MoO_3 are mainly observed in the XRD diagram of these two samples after treatment at 823 K. The X-ray diffractograms of the samples with $ZrO_2 \geq 5\%$ heated to 823 K did not show a peak for the MoO_3 phases. The molybdenum oxide is either amorphous or composed of crystallites smaller than 4 nm. This means that the presence of zirconia on silica favors the dispersion of supported molybdenum species through some interaction with zirconium. Furthermore, this interaction generates a new compound on the surface of Zr(x)SiO_2, as suggested by the XRD pattern of the HPMo/Zr(17)SiO_2 sample calcined at 923 K. All of the peaks of the XRD pattern of this compound correspond to $Zr(MoO_4)_2$ (JCPDS file no. 38-1466).

3.3. IR Spectra. The IR spectra of HPMo supported on SiO_2 and Zr(x)SiO_2 are presented in Figures 2 and 3. For comparative purposes, the IR spectrum of bulk HPMo is shown in Figure 2A. The IR spectrum of fresh bulk HPMo (Figure 2A, line a) shows bands at 1063, 961, 871, and 783 cm^{-1} corresponding to the ($P-O_d$), ($Mo-O_d$), ($Mo-O_b-Mo$), and ($Mo-O_c-Mo$) asymmetric stretching vibrations, respectively, that are characteristic of the Keggin unit.[26,27] The silica support shows three intense IR bands at ca. 1100 (broad and very strong), 800 (medium), and 470 cm^{-1} (strong) (Figure 2B). The silica support partly obscures the HPMo bands, thus hindering the IR characterization. Subtraction of the absorption of silica can induce some artifact bands in the 1200−100 cm^{-1} region due to the strong contrast between the weak signals of the deposited species and the very intense signals of the support. It should also be noted that the IR spectrum of the supported sample resembles that produced by superposition of the spectra of the bulk HPMo and that of silica. The presence of an intense IR absorption band of silica at 804 cm^{-1} and of the HPMo phase at 783 cm^{-1} results in an intense band near 793 cm^{-1} (Figure 2B, line a). The 1063 cm^{-1} band assigned to the ($P-O_d$) asymmetric vibration is significantly masked by the strong silica band at 1100 cm^{-1}. Therefore, the Keggin unit could only be characterized by the highest frequencies at 961 and 871 cm^{-1} (Figure 2B, line a). The IR spectrum of HPMo supported on silica at 283 K shows that the Keggin structure is essentially preserved on the support after impregnation, as evidenced by the agreement between the IR bands of the pure and supported HPMo.

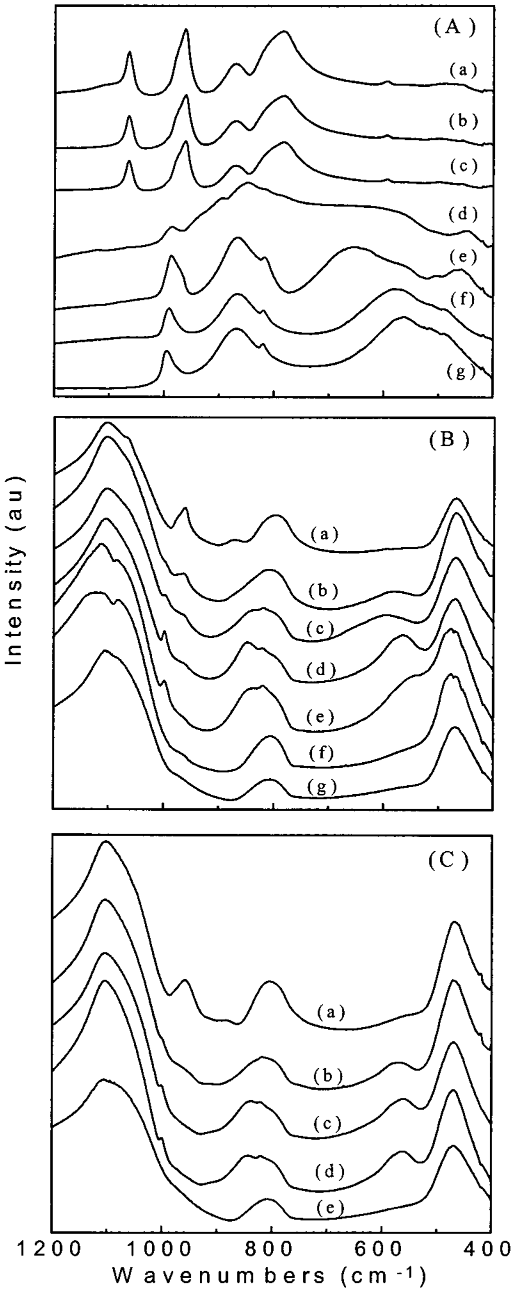

Figure 2. IR spectra of bulk HPMo (A), HPMo/SiO_2 (B), and HPMo/Zr(1.6)SiO_2 (C) calcined at different temperatures. Part A was read at (a) 283, (b) 383, (c) 573, (d) 623, (e) 723, (f) 823, and (g) and 923 K. Part B was read at (a) 283, (b) 523, (c) 623, (d) 723, (e) 823, and (f) 923 K and (g) with SiO2 support. Part C was read at (a) 283, (b) 523, (c) 623, and (d) 723 K and (e) with Zr(1.6)SiO2 support.

After the incorporation of a small amount of zirconium to the silica support, the IR bands of HPMo changed slightly (Figure 2C). The IR bands at 783 and 871 cm^{-1} shifted to higher wavenumbers with increasing zirconium content (to 808 and 878 cm^{-1}, respectively), and the 961 cm^{-1} band shifted to lower wavenumber (to 953 cm^{-1}) (Figure 3A,B, a lines). The presence of a signifi-

---

(25) Fournier, M.; Aouissi, M.; Rocchiccioli-Deltcheff, C. *J. Chem. Soc., Chem. Commun.* **1994**, 307.

(26) Rocchiccioli-Deltcheff, C.; Fournier, M.; Franck, R.; Thouvenot, R. *Inorg. Chem.* **1983**, *22*, 207.

(27) Rocchiccioli-Deltcheff, C.; Fournier, M. *J. Chem. Soc., Faraday Trans.* **1991**, *87*, 3913.

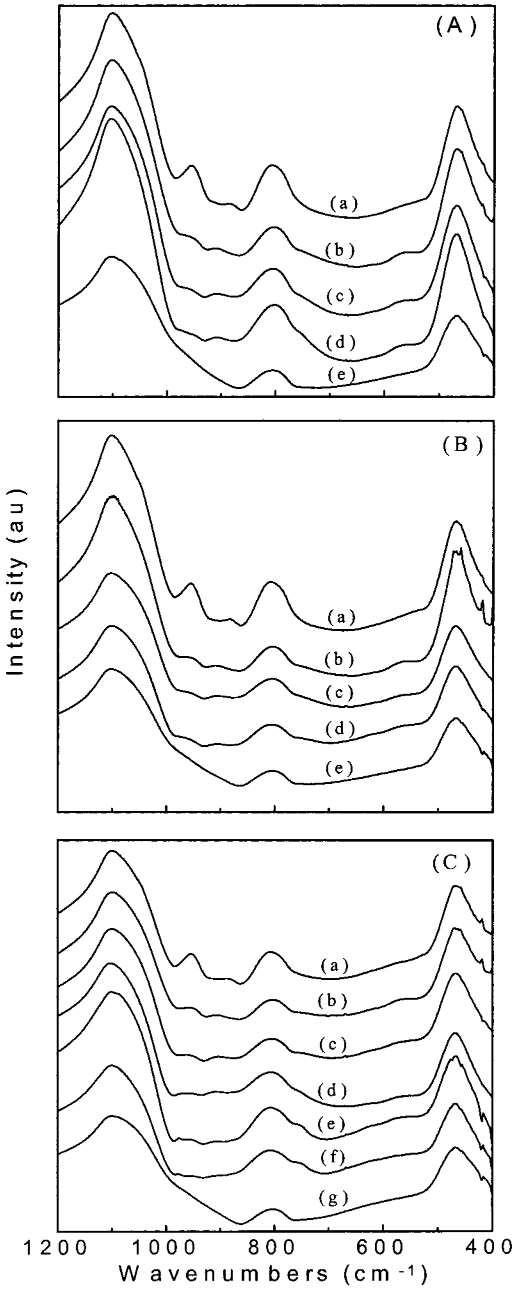

Figure 3. IR spectra of HPMo/Zr(5.6)SiO_2 (A), HPMo/Zr(9.6)-SiO_2 (B), and HPMo/Zr(17.0)SiO_2 at different temperatures. Part A was read at (a) 298, (b) 523, (c) 623, and (d) 723 K and (e) with Zr (5.6)SiO_2 support. Part B was read at (a) 298, (b) 523, (c) 623, and (d) 723 K and (e) with Zr(9.6)SiO_2 support. Part C was read at (a) 298 (b) 523, (c) 623, (d) 723, (e) 823, and (f) 923 K and (g) with Zr(17) SiO_2 support.

cant distorted PO_4 tetrahedron in the sample with the highest Zr content was revealed by a slight shoulder at about 1040 cm^{-1} on the low-wavenumber side of the intense silica band at 1100 cm^{-1} (Figure 3C, line a). These phenomena can be associated with the loss of symmetry of the heteropolyanion structure,[27] due to the increasing anion-support interaction on the zirconia-containing silica support. This is in keeping with previous observations by ^{31}P NMR, which showed that part of the supported HPMo acid is perturbed by an interaction between the acidic protons and the basic surface OH groups and Zr atoms.[28]

The intensity and position of the bands changed after the samples have been subjected to different calcination temperatures. The temperature treatments decreased the intensity and broadened the Keggin unit bands. For the bulk sample, the typical Keggin pattern is preserved up to 573 K, although slight modifications in the band intensity and frequency were observed with respect to the initial spectrum: a change in the relative intensities of the bands at 960 and 1063 cm^{-1} and a broadening of the (Mo$-O_b-$Mo) asymmetric bond vibration (Figure 2A). A broadening of the IR spectra at 623 K was observed for bulk HPMo, indicating a strong disorder in the heteropolyanion and a transformation to molybdenum oxides. Further heating to 873 K resulted in the appearance of α-MoO_3 bands at 993, 882, and 814 cm^{-1} as a consequence of the loss of the Keggin structure. Treatment of the supported samples at 523 K also elicited a decrease in band intensity at 960 cm^{-1}. The (Mo$-O_b-$Mo) asymmetric vibrations for HPMo/SiO_2 and HPMo/Zr(1.6)SiO_2 samples were obscured by the broad band in the 880$-$760 cm^{-1} region (Figure 2B,C). The 878 cm^{-1} band for Zr(x)SiO_2 samples was shifted to 910 cm^{-1} with temperature. This latter could be related to the vibrations of Mo=O bonds in MoO_4^{2-} tetrahedra.[29,30] The bands at 998, 845, 818, and 910 cm^{-1} and 600$-$520 cm^{-1} of α-MoO_3 appeared in the spectra of HPMo/SiO_2 and HPMo/Zr(1.6)SiO_2 samples calcined at 623 K. The 961 cm^{-1} band was present in these samples up to 723 K treatment, meaning that the Keggin unit structure was partly preserved. The intensities of α-MoO_3 bands increase after treatment at 723$-$823 K, due to the formation of the crystalline phase. The bands at 1122, 1080, and 960 cm^{-1} at 923 K from phosphate groups[31] appeared in the spectrum of HPMo/SiO_2. In addition, the MoO_3 bands disappeared. This suggests that the new molybdophosphate species are formed at a higher temperature on the silica surface.

It was difficult to define clear IR peaks of Keggin unit within the 523$-$723 K range for the HPMo/Zr(x)SiO_2 samples (x from 5.6 to 17.0) (Figure 3A$-$C), probably due to an “amorphization” of the heteropolyanion phase or its decomposition. The bands of MoO_3 were not observed in the spectra of these samples, probably owing to the better dispersion of molybdenum species on the Zr(x)SiO_2 supports. The bands at about 747 cm^{-1} in the spectra of HPMo/Zr(17.0)SiO_2 at 623$-$923 K can be assigned to the formation of Zr$(MoO_4)_2$ phase, as suggested by XRD patterns.

3.4. Raman Spectra. The Raman spectra of the bulk HPMo and HPMo/Zr(x)SiO_2 samples are shown in Figures 4 and 5 as a function of the calcination temperature (up to 923 K). The bulk HPMo and HPMo/Zr-(x)SiO_2 samples at 373 and 323 K, respectively, exhibit Raman bands characteristic of the heteropolyanion with Keggin structure[26,27] (Figure 4A,B, a lines). The strong band at 1006 cm^{-1} with a shoulder at 993 cm^{-1} can be attributed to the (Mo$-O_d$) symmetric and (Mo$-O_d$)

---

(28) Damyanova, S.; Fierro, J. L. G.; Sobrados, I.; Sanz, J. *Langmuir* **1998**, in press.

(29) Dufresne, P.; Payen, E.; Grimblot, J.; Bonnele J. P. *J. Phys. Chem.* **1981**, *85*, 2344.

(30) Damyanova S.; Spojakina, A. In *Proceedings of the 7th International Symposium Heterogenous Catalysis*; Bourgas, Bulgaria, 1991; p 1081.

(31) Spojakina, A.; Damyanova, S.; Petrov, L.; Vit, Z. *Appl. Catal.* **1989**, *56*, 163.

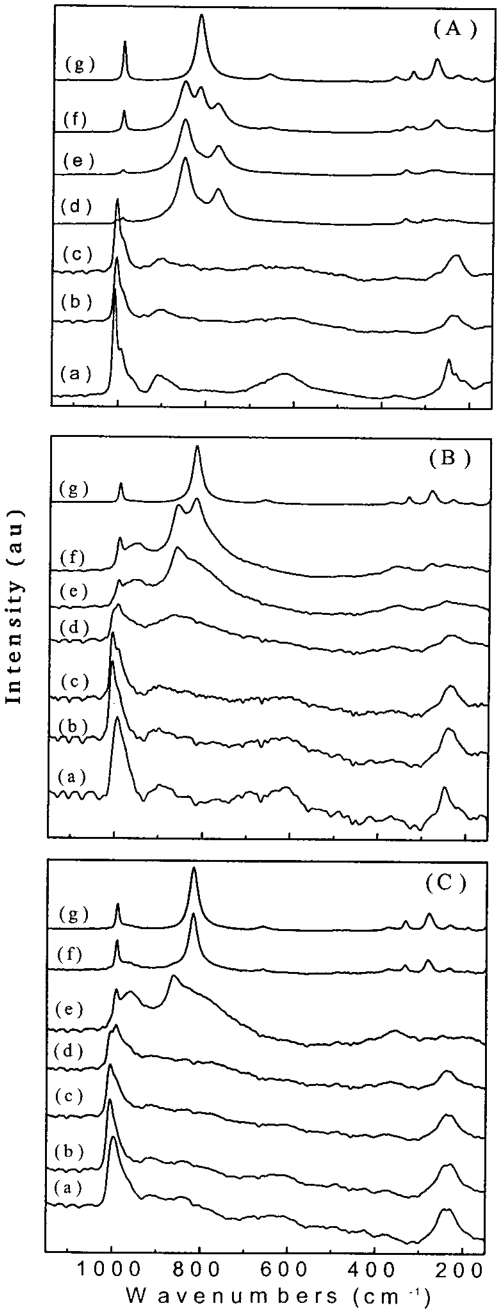

Figure 4. Raman spectra of bulk HPMo (A), HPMo/SiO$_2$ (B), and HPMo/Z(1.6)SiO$_2$ (C) treated at different temperatures. Part A was read at (a) 373, (b) 573, (c) 623, (d) 673, (e) 723, (f) 773, and (g) 823 K. Part B was read at (a) 323, (b) 523, (c) 623, (d) 723, (e) 773, (f) 823, and (g) 923 K. Part C was read at (a) 323, (b) 423, (c) 523, (d) 623, (e) 723, (f) 823, and (g) 923 K.

asymmetric stretching modes of the terminal Mo═O bonds, respectively. The broad bands in the 920−870 and 620−590 cm^{-1} regions can be related to the (Mo−O−Mo) asymmetric and (Mo−O$_c$−Mo) symmetric stretching modes of bridging Mo−O−Mo bonds, respectively.[26,27] The strong band at 248 cm^{-1} corresponds to stretching mode νs(Mo−O$_a$) with an important bridging stretching character; the oxygen links the Mo and the central heteroatom.[26]

Comparison of the Raman spectra of the HPMo/SiO$_2$ sample with the corresponding HPMo/Zr(x)SiO$_2$ samples after impregnation revealed a change in intensity and position (Figures 4C, 5). The terminal Mo═O stretching band was located in the 1010−930 cm^{-1} region. The highest wavenumber value of this band was observed for HPMo/SiO$_2$ sample (1006 cm^{-1}). The asymmetric nature of the terminal bond implies an unresolved shoulder on the lower wavenumber side, which is more pronounced in HPMo/Zr(x)SiO$_2$ samples. The samples with higher Zr content showed broad bands at 912 and 840 cm^{-1} (Figure 5). The presence of these bands could correspond to a partially degraded heteropolyanions, as will be discussed below. As the zirconia coverage increased, the broad band in the region 650−590 cm^{-1} became less pronounced (Figure 5B,C,a). Moreover, the frequency of the 248 cm^{-1} band decreased after the HPMo had been supported, which was more evident for Zr(x)SiO$_2$ support (from 244 cm^{-1} for the silica-sup-

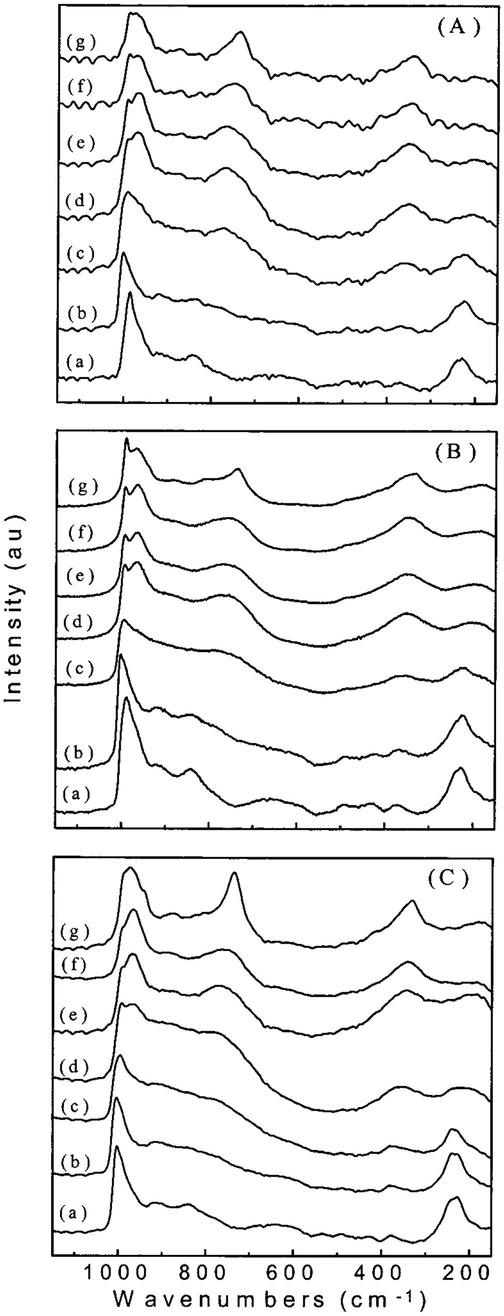

Figure 5. Raman spectra of HPMo/Zr(5.6)SiO$_2$ (A), HPMo/Zr(9.6)SiO$_2$ (B), and HPMo/Zr(17.0)SiO$_2$ (C) at different temperatures: (a) 323, (b) 423, (c) 523, (d) 623, (e) 723, (f) 823, and (g) 923 K.

ported to 233 cm^{-1} for HPMo/Zr(17.0)SiO$_2$ sample). The latter observation suggests the presence of a highly distorted structure that would be due to some interaction between the heteropolymolybdate anion and the support. The different spectra observed for HPMo/Zr-(x)SiO$_2$ series after impregnation may correspond to HPMo interacting with the support.

A shift of the main band to lower wavenumbers (from 1007 to 1004 cm^{-1}) was observed in the spectra of bulk HPMo with increasing calcination temperature up to 573 K, suggesting a shortening of the Mo=O bond under dehydration (Figure 4A). The partial degradation of HPMo units was supported by a shift of the band from 248 to 235 cm^{-1}. The presence of the shoulder at about 991 cm^{-1} suggests the presence of dehydrated molybdenum oxide species. The most significant change in the spectra of HPMo was observed at 673 K treatment (Figure 4). Very small traces of the bands at 1004 and 990 cm^{-1} and a complete disappearance of the (Mo−O$_a$) symmetric stretching mode at 248 cm^{-1} were observed, indicating transformation of the molybdophosphate anion and molybdenum oxide species. New, intense bands at 851 and 775 cm^{-1}, closely resembling those of the β-MoO$_3$ phase,[24] were clearly visible. Well-defined peaks from a mixture of the β- (851, 775 cm^{-1}) and α-MoO$_3$ (990, 818, 281, and 146 cm^{-1}) phases appeared upon calcination at 773 K. It should be stressed here that Fournier et al.[25] observed the β-MoO$_3$ phase even after thermal treatment at 523 K. The same was observed by Rocchiccioli-Deltcheff et al.,[27] but in their case, the bands from α-MoO$_3$ phase appeared at lower temperature (673 K). Larger bands from bulk MoO$_3$ at 990, 816, 661, 375, and 281 cm^{-1} dominated in the 823−923 K range (Figure 4A).

A change in the relative intensities of the bands assigned to the M = O bond at 1007 and 992 cm^{-1} with increasing temperature up to 723 K was observed in the spectra of HPMo/SiO$_2$ sample (Figure 4B). A more significant change at 773 K was observed in the wavenumber, assigned to bridging Mo−O−Mo bonds: the broad band at about 900 cm^{-1} was shifted to about 863 cm^{-1} and a shift from 248 to 234 cm^{-1} in the band assigned to the (Mo−O$_a$) symmetric stretching mode was observed. The HPMo/SiO$_2$ spectra at 823 K (Figure 4B,e) revealed well-resolved peaks at 993, 861, 818 cm^{-1} and a small one at 280 cm^{-1}, meaning that a mixture of α- and β-MoO$_3$ phases is formed at higher temperature than that for the bulk HPMo. This would indicate that supported HPMo is more stable than the unsupported one. A weak band at about 953 cm^{-1} was discerned in samples calcined at 723−823 K but disappeared at higher temperature. Intense bands at 990 and 816 cm^{-1} and weaker ones at 657, 333, and 282 cm^{-1}, associated with the bulk α-MoO$_3$ phase, dominated the spectra at 923 K. The incorporation of a small amount of Zr to the support of the HPMo/Zr(1.6)SiO$_2$ sample scarcely modified the spectra of the Zr-free counterpart. It should be noted that the intensity of the 965−973 cm^{-1} band of the sample calcined at 773 K is higher than that of HPMo/SiO$_2$, and does not disappear completely at higher temperatures.

For samples containing Zr ≥ 5.6 wt %, the stretching mode of the terminal Mo=O bond shifted from 1003 to 1000 cm^{-1} to 996−992 cm^{-1} with the simultaneous appearance of some bands close to 765 and 350 cm^{-1} in samples calcined at 523 K (Figure 5). The presence of the broad band at about 225 cm^{-1} suggests that the polymolybdate anions are present on the surface of Zr-(x)SiO$_2$ supports. New changes were observed upon increasing calcination temperature from 623 to 923 K. The 225 cm^{-1} band disappeared and the intensity of the bands close to 970, 770, and 360 cm^{-1} increased with increasing temperature. A new band near 992 cm^{-1} increased with both the calcination temperature and the Zr content. This band could be assigned to isolated molybdenum oxide species on zirconia.[32,33] Because these species are sensitive to hydration, the Raman spectra of a representative sample was run under hydrated and dehydrated conditions (Figure 6). Upon hydration, the band near 993 cm^{-1} was replaced by new features close to 956 and 878 cm^{-1}: these are characteristic of hydrated molybdenum species in the presence of zirconia.[38] The Raman bands close to 967, 763, 350, and 205 cm^{-1} were not affected by the hydration and must correspond to the new phase, Zr(MoO$_4$)$_2$ detected by XRD. Conversely to silica-supported HPMo, the Zr(x)SiO$_2$ supports break HPMo into surface-dispersed molybdenum oxide species and Zr(MoO$_4$)$_2$ upon heating but did not form the MoO$_3$ phase.

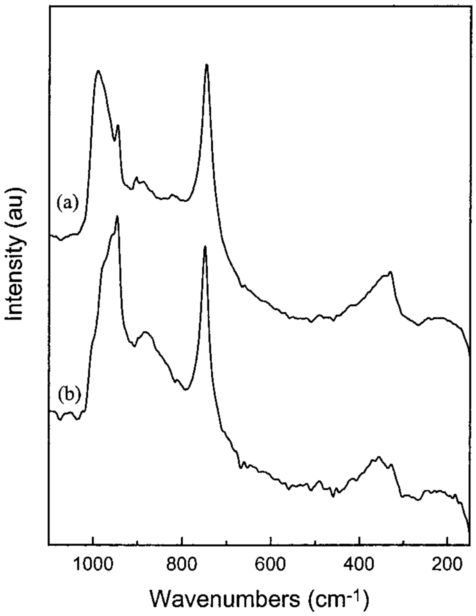

Figure 6. Raman spectra of HPMo/Zr(9.6)SiO$_2$ sample treated at 873 K under dehydrated conditions at 473 K (a) and under hydrated conditions at ambient temperature (b).

3.5. Catalytic Activity. Blank experiments were carried out with the empty reactor without any detectable methanol conversion. Blank experiments with the Zr(x)SiO$_2$ supports were also performed, but no measurable conversion was observed at temperatures below 523 K. The effect of zirconia loading on the catalytic behavior of HPMo/Zr(x)SiO$_2$ samples was studied. The rate of methanol transformation, expressed as millimole of methanol converted per hour and gram of catalyst, at 503 K, is plotted in Figure 7 as a function of Zr loading. The samples selected for this comparison were those calcined at 723 K. The main products observed from methanol oxidation were dimethyl ether (DME), formaldehyde (FA), and methyl formate (MF). The rate increased progressively with increasing Zr content,

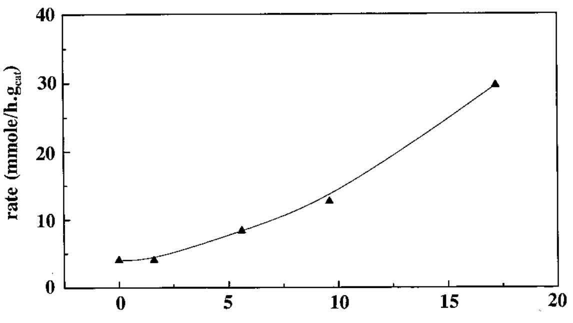

Figure 7. Influence of the Zr content on the rate of methanol oxidation at 503 K over catalysts calcined at 723 K.

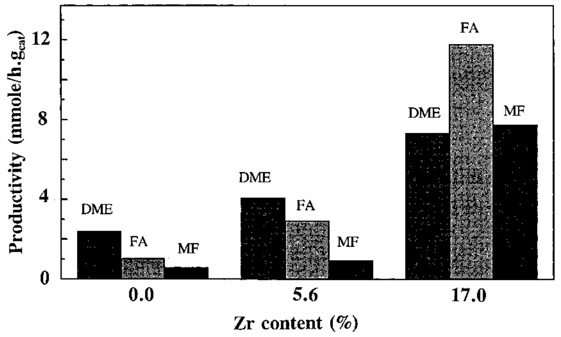

Figure 8. Productivities of major products in the reaction of methanol oxidation at 503 K for representative catalysts calcined at 723 K.

reaching the maximum value for sample HPMo/Zr(17.0)SiO_2, which, in turn, was around 7 times higher than that for the Zr-free counterpart.

Changes in the productivity (mole of a given product produced per hour and gram of catalyst) to DME, FA, and MF over three representative HPMo/Zr(x)SiO_2 (x = 0.0, 5.6, 17.0) samples, calcined at 723 K, are compared in Figure 8. Productivities to a given product increased with the Zr content, and selectivity was found also to depend on the Zr content. Thus, for HPMo/SiO_2 and HPMo/Zr(5.6)SiO_2 samples, selectivity followed the order DME > FA > MF; however, this trend was reversed for HPMo/Zr(17.0)SiO_2 sample. For this latter sample, DME and MF selectivities reached the same level but approximately 40% lower than the FA selectivity. This result indicates a higher dehydrogenation selectivity (FA formation) for the catalyst with the highest Zr loading.

4. Discussion

4.1. Surface Structure of Supported HPMo. Characterization of the supported HPMo under ambient conditions demonstrates that supported heteropolyanion becomes slightly distorted due to interaction with the support. These differences are even more patent with Zr(x)SiO_2 supports. The decrease of the main Raman band frequency assigned to terminal Mo=O bonds and the shift of νs(Mo−O$_a$) mode to lower frequency in supported HPMo points to the shortening of the Mo−O bonds due to dehydration.[26,27] The interaction between the HPMo and the OH groups of the support could have an acid−base nature. Similar to the observation for $H_4SiMo_{12}O_{40}/SiO_2$[33] and $H_3PMo_{12}O_{40}/SiO_2$,[34] some acidic protons from a part of $H_3PMo_{12}O_{40}$ structure could be trapped on the basic OH groups and form positively charged Si(Zr)−OH$^+$ or Si(Zr)−OH$_2^+$ groups able to attract the isolated phosphomolybdate anion through electrostatic interaction and act as a counterion for the heteropolyanion: (Si(Zr)OH$_2^+$)($H_2PMo_{12}O_{40}^-$). It should be noted that this interaction is stronger on Zr(x)SiO_2 than on SiO_2 and a significant disorder of the heteropolyanion symmetry caused by the support is expected for Zr(x)SiO_2 supports.

In solution, heteropolyanions are not stable at pH > 1 and degrade into less polymerized species such as $PMo_{12}O_{40}^{3-} \rightleftarrows PMo_{11}O_{39}^{7-} + MoO_4^{2-} + 6H^+$ as reported by McGarvey and Moffat.[35] Under ambient conditions, oxide supports are hydrated. The point of zero charge (PZC) is determined by both the oxide support and the supported phase. The PZC on silica is 3.7−4.3, and it is 5.9−6.1 on ZrO_2.[32] Thus, the Zr-loaded silica supports must have a higher pH at PZC than silica. The higher pH imposed by Zr(x)SiO_2 supports must afford a more extensive degradation of the heteropolyanion on Zr(x)SiO_2 than on SiO_2. This can be seen in the XRD patterns and in the modifications of the Raman spectra, which show the less intense degree of degradation for the silica-supported heteropolyanion. Owing to this degradation, part of the structural water is lost.[26,27] The presence of compounds with different content of water molecules has also been seen through different chemical shifts in ^{31}P NMR parameters.[28] The structural changes of the hydrated molybdenum oxide species on different mixed-oxide supports with increasing zirconium content confirm the dependence of the supported molybdophosphate heteropolyanion on the zirconium content, which corresponds to the changes in the PZC of the samples. This effect may also be responsible for the decomposition of heteropolyanions during their impregnation on basic supports.[10−13]

The changes in the intensity and the position of the IR and Raman bands and the XRD patterns with calcination temperature suggest that the supported or bulk molybdophosphate anions are thermally sensitive. It appears that the thermal stability of HPMo supported on silica surface is improved in comparison with that of bulk HPMo. The supported heteropolyanion on silica is preserved up to 723 K: i.e., 100 K above bulk HPMo (623 K). This can be ascribed to a very weak interaction with the silica support and, consequently, to the dehydration mechanism during sample heating. Different effects have been reported to be responsible for the modification of the structure of the heteropoly compounds:[25,26] (i) H-bonding through the water molecules or the hydroxonium ions, H_3O^+, which induces a decrease in frequency, and (ii) electrostatic anion−anion interactions, leading to an increase in frequency. Dehydration of the samples “undresses” the hydrated protons and weakens the H bonding. As a consequence, an increase in the (Mo−O$_t$) symmetric mode is observed in the spectra of bulk and silica-supported HPMo. The symmetry of the heteropolyanion is perturbed by the loss of crystallization water, and the (Mo−O$_a$) symmetric

---

(32) Hu, H.; Wachs, Y. E.; Bare, S. R. *J. Phys. Chem.* **1995**, *99*, 10899.

(33) Thouvenot, R.; Fournier, M.; Rocchiccioli-Deltcheff, C. *J. Chem. Soc., Faraday Trans.* **1991**, *87*, 2829.

(34) Lefebre, F. *J. Chem. Soc., Chem. Commun.* **1992**, 756.

(35) McGarvey, G. B.; Moffat, J. B. *J. Mol. Catal.* **1991**, *69*, 137.

Table 3. Surface Atomic Ratios of Samples HPMo/Zr(x)SiO$_2$ Subjected to Different Calcination Temperatures

sample	Mo/Si at	Zr/Si at	Mo/(Zr + Si)	P/Si
		383 K		
PMo/SiO$_2$	0.039		0.039	0.005
PMo/Zr(5.6)SiO$_2$	0.041	0.040	0.039	0.004
PMo/Zr(17.0)SiO$_2$	0.126	0.303	0.097	0.004
		523 K		
PMo/SiO$_2$	0.053		0.053	
PMo/Zr(5.6)SiO$_2$	0.060	0.040	0.057	
PMo/Zr(9.6)SiO$_2$	0.074	0.075	0.063	
PMo/Zr(17.0)SiO$_2$	0.150	0.318	0.114	
		623 K		
PMo/SiO$_2$	0.076		0.076	0.002
PMo/Zr(5.6)SiO$_2$	0.064	0.032	0.062	
PMo/Zr(9.6)SiO$_2$	0.064	0.057	0.060	
PMo/Zr(17.0)SiO$_2$	0.156	0.334	0.117	
		723 K		
PMo/SiO$_2$	0.127		0.127	0.003
PMo/Zr(5.6)SiO$_2$	0.055	0.026	0.054	
PMo/Zr(9.6)SiO$_2$	0.067	0.048	0.064	
PMo/Zr(17.0)SiO$_2$	0.135	0.305	0.103	

mode decreases (Figures 3 and 4). The anhydrous phase of HPMo is formed after elimination of crystallization water within the 393−503 K range in agreement with the decrease of the BE of Mo 3d$_{5/2}$ core level and the DTG and DTA data.[19] This phase consists of an isotropic distribution of protonated KU in the framework[26] and is stable within the 393−603 K range.[19] In addition, it has been found[36,37] that the bridging oxygen atoms connecting two trimolybdic groups may be the most highly charged atoms of the polyanions and the protons would be localized on them. The latter is revealed by a decrease and broadening of (Mo−O$_b$−Mo) Raman asymmetric mode with changes in the degree of dehydration of the samples with increasing temperature (Figures 4 and 5). The broad ^{31}P NMR resonance, with chemical shifts of (−3.5) to (−3.8) ppm at 383−473 K for HPMo and HPMo/SiO$_2$,[28] has also been associated with the localization of the acidic protons near the bridging Mo−O−Mo oxygen and formation of the anhydrous phase with preserved KU. From XPS data, it appears that HPMo is relatively well dispersed on the silica surface in the 383−623 K range. This again suggests that there is an interaction of the HPA and some sites of the silica surface that stabilizes the molybdophosphate anions with a preserved KU. The changes in frequency reflect a gradual dehydration of the HPMo and HPMo/SiO$_2$ and their transformation into a mixture of α- and β-MoO$_3$ phases and that the former dominates at higher temperatures. In the 773−923 K range, molybdophosphates are formed on the silica surface.

4.2. Effect of Zr on Catalyst Structure and Performance. It should be noted that the interaction between the molybdophosphate anion and the support is higher for HPMo/Zr(x)SiO$_2$ supports, as is revealed by the constant values of XPS Mo/(Zr + Si) atomic ratios (Table 3). The addition of a small amount of Zr (1.6 wt %) has little effect on the spectra of the samples in comparison with the Zr-free counterpart. However, the higher Zr contents lead to the transformation of HPMo at lower temperatures: a decrease in the frequency of the terminal Mo═O bonds and of the (Mo−O$_a$) symmetric mode. These point to a stronger affinity of Zr for the HPMo phase, mainly at high calcination temperatures, because the bands of the KU disappear and new bands become dominant. These bands close to 340, 747, 947, and 975 cm^{-1} are not sensitive to hydration, which suggest the formation of a new compound. In fact, these new bands must correspond to the Zr(MoO$_4$)$_2$ phase detected by XRD for these samples. At intermediate temperatures, the bands are broader and shifted to higher wavenumbers (350, 763, and 967 cm^{-1}). It is expected that these bands would reflect the incipient formation of Zr(MoO$_4$)$_2$ with an ill-defined structure. There is also a Raman band near 990 cm^{-1} that is sensitive to hydration and corresponds to isolated molybdenum oxide species.[38,39] Thus, the original HPMo breaks down into phosphates and molybdenum oxide, and some of the Mo sites react with surface zirconia, affording the Zr(MoO$_4$)$_2$ phase. The solid-state reaction between Mo and Zr is facilitated by increasing both calcination temperature and Zr loading.

The increase of the rate of methanol oxidation with the Zr loading (Figure 7) cannot be explained in terms of the catalyst texture because the specific areas follow an opposite trend (Table 1). Besides that, the absence of any correlation between XPS Mo/Si or Mo/(Si + Zr) atomic ratios (Table 3) and reaction rate suggests that zirconium oxide species, which cover a fraction of the silica surface and interact with molybdenum oxide species, resulting from partial or complete degradation of the molybdophosphate anions, are responsible of the activity enhancement. According to the established mechanism of the methanol dehydration on oxide catalysts,[40,41] the main step is formation of methoxide intermediate on the acid sites. This intermediate can either react with another CH$_3$OH molecule to form DME (acid−base reaction) or undergo a nucleophilic attack of surface oxide ion to form an FA precursor (redox reaction). Therefore, it could expected that the proportion of acid−base/redox sites on the catalysts would control the selectivity of the overall reaction. The marked decrease of the DME/FA selectivity ratio (Figure 8) with increasing zirconium content on the samples calcined at 723 K indicates clearly that Mo−Zr interaction species are responsible for the enhancement of FA selectivity. The high selectivity of the HPMo/SiO$_2$ catalyst for DME suggests that there are available protons on the catalyst able to protonate methanol. It is inferred that these Brönsted acid sites are linked to the heteropolyanion on the Zr-free silica surface.

SiO$_2$- and Zr(x)SiO$_2$-supported HPMo behave quite differently upon heating. On silica, HPMo breaks apart into phosphates and bulk MoO$_3$. The interaction with silica support is so weak that no surface molybdenum oxide is formed. By contrast, zirconia does show higher affinity for Mo sites. Thus, on Zr(x)SiO$_2$ supports, HPMo breaks down at a temperature lower than that on silica and forms molybdenum oxide species. The affinity

---

(36) Barrous, J. N.; Jameson, G. B.; Pope, M. T. *J. Am. Chem. Soc.* **1985**, *107*, 1771.

(37) Mastikhin, V. M.; Kulikov, S. M.; Nosov, A. V.; Kozhevnikov, Y. V.; Mudrakovsky, Y. L.; Timofeeva, M. N. *J. Mol. Catal.* **1990**, *60*, 65.

(38) Bañares, M. A.; Hu, H.; Wachs, I. E. *J. Catal.* **1994**, *150*, 407.

(39) Kim, D. S.; Wachs, I. E.; Segawa, K. *J. Catal.* **1994**, *146*, 268.

(40) Weber, R. S. *J. Phys. Chem.* **1994**, *98*, 2999.

(41) Tatibouët, J. M. *Appl. Catal. A: Gen.* **1997**, *148*, 213.

between both oxides facilitates the formation of Zr(MoO_4)$_2$ phase. As expected, the extent of this solid-state reaction increases with temperature. Increasing amounts of zirconium also leads to a more marked production of the new phase, as suggested by the 990/979 cm^{-1} Raman band intensity ratios.

5. Conclusion

Study on the structural changes of supported HPMo at different temperatures reveals significant differences, depending on the specific support used. Under ambient conditions, a moderate degradation of HPMo is observed on silica, whereas this is stronger on $Zr(x)SiO_2$ supports due to the high pH at PZC on Zr-containing supports. Silica increases the thermal stability of HPMo, as compared to the bulk HPMo. Conversely, zirconia is more reactive and decreases the breakage temperature of HPMo; the stabilization of surface Mo−oxide species must be the driving force underlying this. The interaction is so intense that the compounds react to form the $Zr(MoO_4)_2$ phase, as is observed by XRD and is suggested by Raman spectroscopy. On silica, the interaction is so weak that no surface molybdenum oxide can be destabilized because it segregates as β-MoO_3, which is converted into α-MoO_3. The presence of this Mo−Zr species appear to be responsible for the activity enhancement in methanol oxidation. The marked decrease of the DME/FA selectivity ratio with increasing zirconium content on the samples calcined at 723 K indicates that the redox function of the Mo−Zr species improves FA selectivity.

Acknowledgment. S.D. thanks the Spanish Ministry of Education and Culture for a sabbatical year grant. Financial support from the CICYT, Spain, under Projects QUI98-0877 and CICYT IN96-0053 is also acknowledged. The authors are indebted to Prof. M. A. Bañares-Muñoz (University of Salamanca, Spain) for valuable comments on XRD.

CM9911316